

# Improving Shoreline Forecasting Models with Multi-Objective Genetic Programming

Mahmoud Al Najar<sup>a,b,\*</sup>, Rafael Almar<sup>a</sup>, Erwin W. J. Bergsma<sup>c</sup>, Jean-Marc Delvit<sup>c</sup> and Dennis G. Wilson<sup>b</sup>

<sup>a</sup>Laboratory of Spatial Geophysics and Oceanography Studies (CNES/CNRS/IRD/UPS), University of Toulouse, Toulouse, France

<sup>b</sup>ISAE-SUPAERO, University of Toulouse, Toulouse, France

<sup>c</sup>Earth Observation Lab, The French Space Agency (CNES), Toulouse, France

## ARTICLE INFO

### Keywords:

Genetic algorithms  
Genetic programming  
Genetic improvement  
NSGA-II  
Shoreline forecasting  
Climate change

## ABSTRACT

Given the current context of climate change and increasing population densities at coastal zones, there is an increasing need to be able to predict the development of our coasts. Recent advances in artificial intelligence allow for automatic analysis of observational data. This work makes use of Symbolic Regression, a type of Machine Learning algorithm, to evolve interpretable shoreline forecasting models. Cartesian Genetic Programming (CGP) is used in order to encode and improve upon ShoreFor, a shoreline prediction model. Coupled with NSGA-II, the CGP individuals are evaluated and selected during evolution according to their predictive skills at five coastal sites. This work presents a comparison between the CGP-evolved models and the base ShoreFor model. In addition to its ability to produce well-performing models, the work demonstrates the usefulness of CGP as a research tool to gain insight into the behaviors of shorelines at different points around the globe.

## 1. Introduction


Coasts around the globe are continuously facing natural and anthropogenic pressures. Our knowledge and understanding of the evolution of the coastal zone over time is crucial for a large variety of applications including coastal risk monitoring and management. Shoreline evolution forecasting is an important element in coastal studies that aims to better understand and predict the occurrence and intensity of erosive and accretive forces. Recently, large efforts have been made to understand and predict shoreline evolution due to the rising social, economic and natural pressures such as climate change [43, 10, 44, 48].

Shoreline change occurs at varying time scales resulting from different natural processes, ranging from small oscillations resulting from individual waves to decadal trends as a response to varying wave climates. At seasonal to interannual scales, cross-shore sediment transport is considered the main driver of shoreline change, while alongshore processes are more relevant at longer timescales [33, 56, 58].

Symbolic Regression (SR) is a domain of Machine Learning (ML) algorithms that search for symbolic representations of the relationships embedded in the data. Evolutionary algorithms, and specifically Genetic Programming (GP), are often used for SR. GP operates by composing a predefined set of functions in a tree, graph, or other structure; the composition of functions is determined by an evolutionary algorithm. As the optimized model is a functional graph or tree, GP is considered an interpretable ML technique that can be used to derive simple symbolic forms of relationships in data. GP has been demonstrated to be competitive with machine learning approaches such as gradient boosting [31] and has been used in many applications like dimensionality reduction [65], particle physics [11, 35], quantum computing [54, 55], wave characteristic prediction [21], and water stream-flow forecasting [38].

This work frames the problem of forecasting cross-shore shoreline change as a data-driven symbolic regression task. We experiment on the use of Cartesian Genetic Programming (CGP) and the Non-dominated Sorting Genetic Algorithm II (NSGA-II) to encode and evolve interpretable shoreline change models. To promote model generalization, the evolved models are optimized to maximize prediction accuracy at five different coastal sites from around the globe. Evolution discovers new shoreline forecasting models which outperform existing physical models on the

\*Corresponding author

 mahmoud.al-najar@isae-supaero.fr (M. Al Najar); rafael.almar@ird.fr (R. Almar); erwin.bergsma@cnes.fr (E.W.J. Bergsma); jean-marc.delvit@cnes.fr (J. Delvit); dennis.wilson@isae-supaero.fr (D.G. Wilson)  
ORCID(s): 0000-0001-7021-132X (M. Al Najar)

individual sites and also across the five studied sites. We analyze two proposed models which perform well generally to demonstrate their explainability.

We next present an overview of symbolic regression and shoreline change forecasting, with a presentation of the ShoreFor [13] forecasting method used as a baseline model for comparison and improvement in this work. We then present the study sites and datasets used in Section 3. The method, a combination of CGP and NSGA-II adapted for genetic improvement, and the implementation of the ShoreFor model as a CGP graph, are presented in Section 4. Finally, we detail the evolutionary multi-objective optimization on the selected sites in Section 4.5 and analyze the highest performing models in Section 5, including two generalist models which outperform ShoreFor across the five sites while being simple and interpretable.

## 2. Related works

### 2.1. Symbolic Regression

Symbolic regression (SR) is a family of ML algorithms that search for mathematical expressions that best describe the relations between the independent input variables and a dependent output variable. The search space is bounded by a predefined set of components including a set of elementary mathematical operators, constants, and input variables. SR algorithms are particularly interesting as research tools as the outputs of these algorithms are arithmetic expressions rather than sets of coefficients, making them highly interpretable, which allows the practitioner to gain insight into the real-world processes embedded in observed datasets in addition to developing powerful prediction models.

SR algorithms appear in a wide array of applications in the literature. SR was used in [47] to predict the dynamics of harmonic and coupled oscillators, as well as the power production of solar panels. In [64, 63], a physics-inspired method for symbolic regression based on neural networks is developed and tested on a set of 100 equations from the *Feynman Lectures on Physics*. [66] applies SR to discover hidden physics in a variety of problems using sparse observation data. Multiple works make use of SR to study the nonlinear changes in the properties of materials in response to external factors [70, 73, 28]. In [79], coarse atmospheric model outputs are downscaled using GP-based SR to higher resolutions in order to be used in land surface and hydrological models. [18] presents an application of SR to discover dimensionally-consistent nonlinear equations for modelling post-fire debris-flow volume discharge. In [40], SR is used to develop a rainfall-runoff model for streamflow forecasting based on multigene genetic programming and moving-average filtering. We refer the interested reader to [45, 31] for comprehensive reviews on SR. A common point among the diverse SR literature is the use of GP as one of the main methods for SR.

Despite its adoption in other domains, the use of SR, and GP in particular, remains relatively unexplored in coastal science. Some of the related works in coastal science making use of GP include [20], where GP is used to perform real-time wave forecasting and is shown to be a promising tool for coastal prediction studies. In [30], GP was successfully used to perform shore-term forecasting of wave heights based on wind speed and direction, and the evolved models were shown to be applicable over physically-similar but previously-unseen sites. [46] makes use of GP to predict swash zone excursion on sandy beaches. The authors compare their GP-based models to existing literature and show that the GP can be used to develop higher performing predictors while gaining insight into the physical processes, demonstrating the use of GP as a strong data analysis tool.

In [22], the authors review a large number of ML applications to coastal problems including sediment transport and coastal morphodynamics. Although some works make use of GP, the majority of existing ML-based literature in the domain make use of Artificial Neural Networks and Bayesian Networks in order to learn predictive models from the data. Here, we make use of Cartesian Genetic Programming (CGP) in a multi-objective optimization scheme using the Non-dominated sorting algorithm (NSGA-II) in order to evolve an existing shoreline forecasting model.

### 2.2. Existing methods in shoreline change forecasting

Three main types of methods have been proposed and discussed in the literature on the topic of forecasting shoreline change [43].

Process-based models include detailed information on the physical processes that happen in the nearshore including wave propagation and dissipation, nearshore currents, sediment transport processes and the resulting changes in the nearshore morphology. These simulated processes are usually coupled through mass and momentum conservation laws. Such models include MIKE 21 [72], Delft3D [34], ROMS [71] and CROCO [39]. In general, these models are used to model short-term and local events in the nearshore zone and are not considered applicable over larger spatio-temporal scales [43, 12].

Hybrid models are mixed approaches to modelling shoreline change incorporating general physical principles, such as the principle of shoreline equilibrium [75], and are calibrated using data-driven approaches (e.g. least-squares-fit). A large number of hybrid models have been developed in the literature [13, 61, 67, 26, 49]. Compared to process-based models, hybrid models can be used to predict shoreline position over much longer time scales, however they are generally unable to generalize to previously-unseen areas and require site-specific field data for model calibration.

Finally, data-driven techniques rely fully on the available dataset in order to learn the physical relationship between the forcing parameters in the input data and the resulting shoreline change as the output. In [78], different types of neural networks are used to model shoreline change and are compared according to their forecast performance. In [7], a variety of neural network models are compared to traditional forecasting techniques as well as ordinary-least-squares (OLS) regression on a global scale using satellite derived shoreline time series. [76] makes use of a daily-scale shoreline time series dataset to compare a statistical forecasting model SARIMA to two ML-based models (NNAR and LSTM) and to EOF analysis as the baseline in tasks of single-step and multi-step forecasting. [53] presents and compares multiple models for coastal erosion prediction at Narrabeen, Australia, including two process-based models, an empirical model and a neural network, in addition to an ensemble of the four models. In [27], neural networks are used in conjunction with genetic algorithms in order to find suitable parameterizations for a coupled process-based model, Windsurf. A neural network is then trained on the task of beach and dune change forecasting using outputs from Windsurf. In [43], a number of shoreline forecasting techniques are applied at Tairua beach in New Zealand in a competition setting. Some of the data-driven techniques included multiple types of Artificial Neural Networks (MLP, Autoregressive NN, LSTM), Bayesian Networks, in addition to more traditional techniques such as K-nearest neighbors and Random Forests. In general, data-driven techniques performed well over familiar conditions and settings, but they failed to generalize to previously-unseen conditions.

Artificial Neural Networks (ANN's) are the most commonly used models in similar works employing AI for shoreline forecasting [22]. While ANN's have helped achieve significant advances in many domains, explaining their predictions remains relatively difficult due to their black-box nature [57, 4]. To our knowledge, this work is the first step towards the use of data-driven symbolic regression in order to evolve interpretable shoreline forecasting models.

### 2.2.1. ShoreFor

ShoreFor [13] is a shoreline change forecasting model that is built upon the principle of shoreline equilibrium [75], where shorelines continuously evolve towards a time-varying equilibrium condition. ShoreFor can be formulated according to Equation 1, where  $dx/dt$  is the rate of shoreline change,  $F$  is the magnitude of wave forcing,  $c$  and  $b$  are model free parameters that are optimized using a least-squares-fit minimizing the root-mean-squared-error (RMSE) of the model.

$$\frac{dx}{dt} = c(F^+ + rF^-) + b \quad (1)$$

The wave forcing term  $F$  (Equation 2) is expressed in terms of the wave energy flux  $P$  and the normalized disequilibrium term  $\Delta\Omega/\sigma_{\Delta\Omega}$ .

$$F = P^{0.5} \frac{\Delta\Omega}{\sigma_{\Delta\Omega}} \quad (2)$$

ShoreFor defines the beach equilibrium state ( $\Omega_{eq}$ , Equation 3) as a weighted average of antecedent dimensionless fall velocities where  $\phi$  is a model-free parameter which controls the number of days in the series used to estimate the current equilibrium state.

$$\Omega_{eq} = \frac{\sum_{i=1}^{2\phi} \Omega_i 10^{-i/\phi}}{\sum_{i=1}^{2\phi} 10^{-i/\phi}} \quad (3)$$

$\Omega$ , calculated according to Equation 4, represents the rate of sedimentation and is a function of the sediment grain settling velocity  $w$ , the breaking wave height  $H_{s,b}$  and wave period  $T_p$ .

$$\Omega = \frac{H_{s,b}}{wT_p} \quad (4)$$

1 Disequilibrium,  $\Delta\Omega = \Omega_{eq} - \Omega$ , is used to partition forcing  $F$  into accretion and erosion ( $F^+$ ,  $F^-$ ) according to  
 2 the sign of  $\Delta\Omega$ . The erosion ratio  $r$  (Equation 5) is defined as a ratio between the detrended accretive and erosive wave  
 3 forcing. It is calculated over the full wave forcing time series and treated as a constant to balance the accretion and  
 4 erosion terms within the ShoreFor model.

$$r = \left| \frac{\sum_{i=0}^N \langle F_i^+ \rangle}{\sum_{i=0}^N \langle F_i^- \rangle} \right| \quad (5)$$

5 ShoreFor has been used in multiple shoreline prediction studies and a number of extensions have been proposed  
 6 to improve its performance by accounting for shoreline change over different time-scales [50] as well as alongshore  
 7 sediment transport processes [59, 60]. We make use of the ShoreFor model as a base for our experiments on the use  
 8 of CGP for shoreline forecasting in a GI setting, and we highlight the possibility of extending the base CGP-ShoreFor  
 9 implementation to account for these additional processes.

### 10 3. Study zones

11 Shoreline datasets from five different sites around the globe covering different coastal settings are used in this work.  
 12 As shown in Figure 1, these sites include the Grand Popo beach in Benin, Gulf of Guinea, in West Africa. Truc Vert  
 13 beach in the Aquitaine region of France. Narrabeen beach on the coastline of the Sydney metropolitan area, on the  
 14 eastern coast of Australia. In addition to two different sites from the USA, Duck NC on the eastern coast, and Torrey  
 15 Pines on the western coast.

16 A mixture of techniques were used to gather these datasets. Video-derived cross-shore shoreline locations are used  
 17 to compose the shoreline time series of Grand Popo and Narrabeen. In-situ GPS surveys were performed to record the  
 18 shoreline positions of the remaining sites (Duck, Torrey Pines, Truc Vert).

19 In-situ techniques (wave-bouys) and modelling were used to create the time series of wave parameters over the five  
 20 sites including significant wave height ( $H_s$ ), peak wave period ( $T_p$ ), and wave direction ( $Dir$ ). These parameters are  
 21 used to compute the  $\Omega$  and  $P$  time series according to [13]. Sea-level anomaly was observed from satellite altimetry over  
 22 all sites, while river discharge was extracted from a global model hindcast (ISBA-CTrip) and represents the regional  
 23 impact of river discharge. We refer the interested reader to the following articles where more detailed descriptions of  
 24 the physical characteristics of these sites are presented: [3, 5, 56].

25 Figure 2 presents the shoreline time series and the associated wave energy flux ( $P$ ) time series used in this work,  
 26 and demonstrates the differences in wave forcing and the resulting shoreline behaviors over the five different coastal  
 27 sites.

28 Given the varying physical conditions and climates between the sites, as demonstrated by the varying performance  
 29 of ShoreFor across sites in Section 5, we make use of the prediction performance at these sites as five competing  
 30 objectives for evolution. We posit that different features contribute to shoreline change over the five sites, and that  
 31 suitable shoreline models will therefore vary between sites. In the results section, we demonstrate the method's ability  
 32 to evolve site-wise experts that perform well at specific sites, in addition to generalist models that achieve competitive  
 33 results compared to ShoreFor across the five different sites.

### 34 4. Methods

35 To find improved shoreline forecasting models on the five sites, we use Cartesian Genetic Programming, a form  
 36 of GP which encodes functions as graph. We encode the original ShoreFor model as a GCP graph for automatic  
 37 improvement. NSGA-II, a genetic algorithm, is then used to improve models over the five sites simultaneously.

#### 38 4.1. Cartesian Genetic Programming

39 Cartesian Genetic Programming (CGP) [41] is a form of genetic programming that encodes programs as directed  
 40 acyclic graphs. An individual CGP graph is composed of three components: input nodes, output nodes and computation  
 41 nodes. To represent a program as a genome, each node in the graph can be associated with integers corresponding to  
 42 the function of the node and its inputs; two-arity functions like  $x + y$  are most common and used here, so each node is  
 43 represented by three integers. These integers are optimized by evolution by constructing a graph which connects output

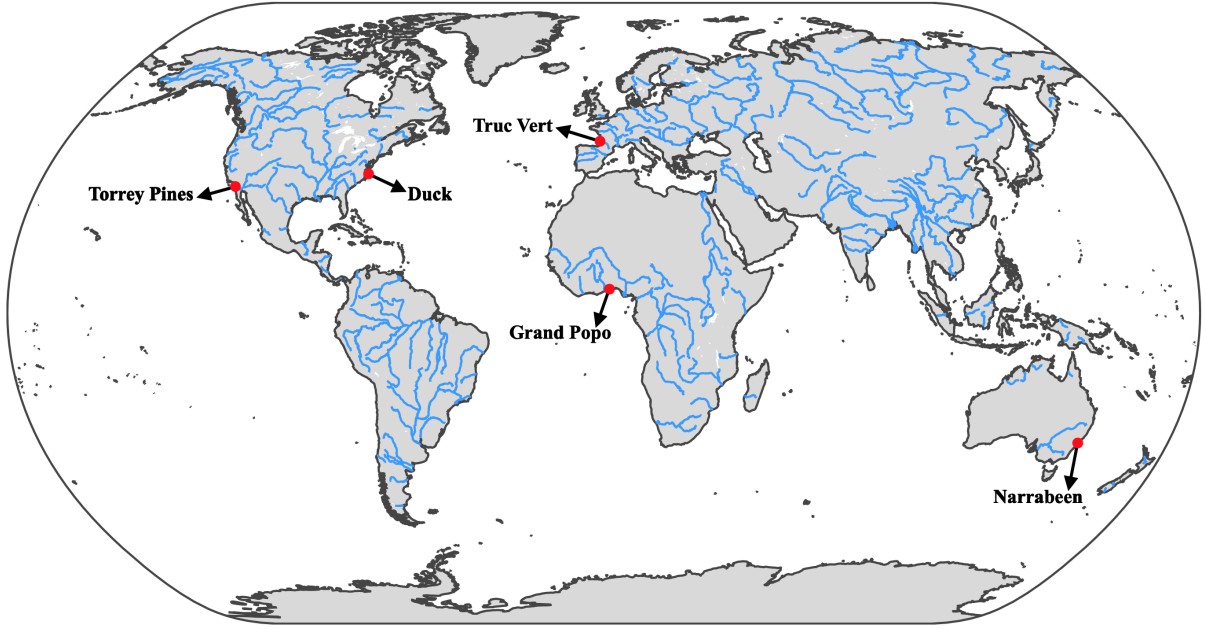


**Figure 1:** World map highlighting the locations of the five sites included in this study.

1 nodes to input nodes and evaluating this graph in an objective function. A CGP genome is of fixed size, however the  
 2 program graph can be of variable size as only a subset of nodes are connected to the output nodes and finally used  
 3 during evaluation. This allows for flexibility in the number of nodes an individual can use, where nodes that do not  
 4 contribute to the output are simply ignored during individual evaluation. CGP has been successfully applied to a large  
 5 number of problems including digital circuit design [9], image processing [51, 24], computer vision-based applications  
 6 [74], among others [42].

7 In this work, we use a mostly standard CGP representation with modifications to optimization for NSGA-II and  
 8 more efficient mutations, and modifications to the function set in order to represent ShoreFor. As in [2], we employ  
 9 the following mutation-level constraints: 1) We discard all mutated graphs with direct input-output connections. 2)  
 10 We ensure that for the same set of random inputs, the outputs produced by parent graph and the mutated graph are  
 11 different in order to minimize the chances of having behaviorally identical individuals in the population. 3) Since we  
 12 use a mixed-type version of CGP where both scalar and vector values exist within the computational graph, we add a  
 13 constraint that discards any mutated graph that outputs scalar values. 4) Finally, we ensure that the size of the output  
 14 vector is equal to the size of the input time series.

#### 15 4.2. Encoding ShoreFor in CGP

16 The use of an established model as an initialization for evolution has been empirically shown to aid in faster  
 17 convergence of the algorithm [2]. We therefore encode the ShoreFor model as a CGP individual in order to improve  
 18 it using evolution. The first population of individuals is created such that the models share the same active graph as  
 19 the ShoreFor individual, and random genes are used to fill in the inactive nodes. The encoding also informs the inputs  
 20 available and the function set, as we use functions during search which are necessary to encode the ShoreFor individual.

21 We first implement equation 3, the  $\Omega_{eq}$  time series, by calculating the weight vector  $W = 10^{-i/\phi}$ , which is  
 22 computed such that the weighting factor decreases per day  $i$  over the number of days  $\phi$ . In order to encode the  
 23 computation of this weight vector, two inputs and five different functions are required; the inputs are the calibrated  
 24  $\phi$  constant and the value of  $2\phi$ , which specifies the size of the moving window. Given these inputs, we decompose  
 25 the calculation of  $W$  as follows. First, a vector of length  $2\phi$  with values ranging from 1 to  $2\phi$  is computed using the  
 26 *irange* function. This vector is then simply flipped using the *reverse* function, to represent the number of days back in  
 27 history each point in the time series represents. At this point, the vector of  $i$  in  $10^{-i/\phi}$  is computed. Then, this vector  
 28 is negated using the *negate* function and divided by the input constant  $\phi$  using *div*, resulting in a vector of values  
 29 representing  $-i/\phi$ . This vector is passed to the *tpow* function ( $tpow(x) = 10^x$ ), obtaining  $W = 10^{-i/\phi}$ . In order to

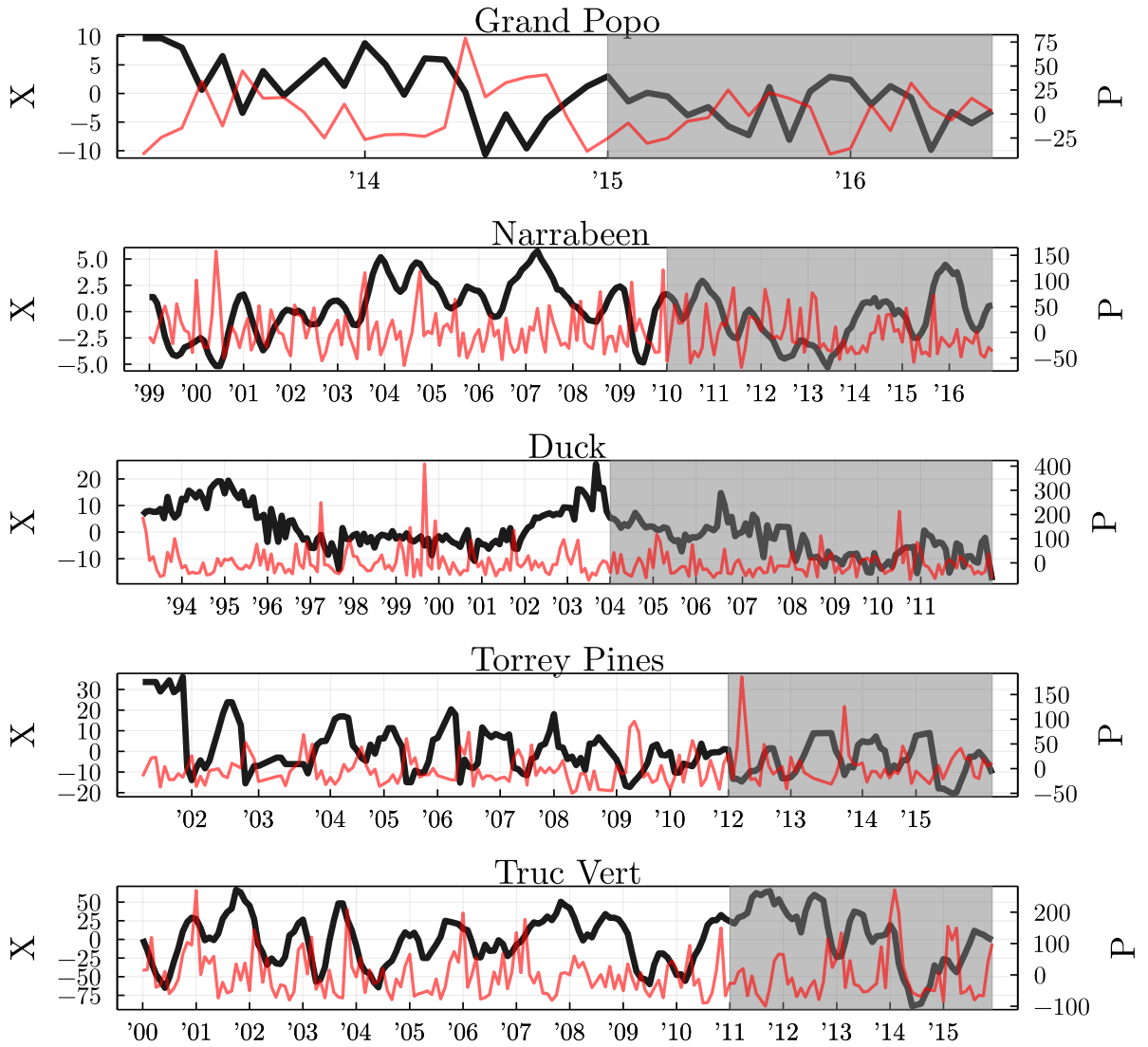


**Figure 2:** Visualization of the shoreline time series from each of the five sites used in this work. Cross-shore shoreline location ( $X$ ) is shown in black. Wave power ( $P$ ) is shown in red. The shaded area corresponds to the forecast period at each site.

1 compute the moving average over the full time series, we make use of the convolution function. We therefore modify  
 2 the computation of  $\Omega_{eq}$  as follows:  $\Omega_{eq} = conv(\Omega, \frac{10^{-i/\phi}}{\sum_{i=1}^{2\phi} 10^{-i/\phi}})$ . The next step in the computational graph is to divide  
 3 the weight vector by the sum of the vector itself to be used as the convolution filter. The graph-form of Equation 3 is  
 4 shown in Figure A.1(left).

5 The final set of inputs used in our CGP-ShoreFor implementation is described in Table 1. We note that not all  
 6 inputs included in our implementation are used by the ShoreFor model. These additional inputs are included so that  
 7 evolution can integrate them into the evolved models.

8 Generally speaking, implementations of CGP require that all input and computed variables are bound to a range of  
 9 -1 to 1 in order to prevent various computational issues such as the existence of NaN's or infinities in the computational  
 10 graph. However, this requirement is difficult to achieve in the case of GI of a physical system of equations due to the  
 11 lack of true maxima for each input and the use of unbounded functions in the original model. Therefore, we instead

**Table 1**

Inputs to the CGP-ShoreFor model. \*Additional inputs that are not used by ShoreFor.

Input	Description
$\Omega$	Dimensionless fall-velocity time series
$P$	Wave power time series
$\phi$	Pre-calibrated number of days used for the initial ShoreFor model
$2\phi$	Used to indicate the size of the weight vector in Equation 3
$D^*$	Wave direction time series
$H_{s,b}^*$	Peak breaking wave height
$T_p^*$	Peak wave period
$S^*$	Sea level anomaly
$R^*$	Regional river discharge

1 choose to handle out-of-bounds computation by penalizing all such individuals by assigning them a fitness value of  
 2 negative infinity, essentially discarding them from future generations.

3 After encoding the ShoreFor system of equations as a single CGP genome, the ShoreFor individual can be  
 4 represented as a graph structure as shown in Figure A.1(right). The ShoreFor graph is used to initialize the active  
 5 graphs of the individuals at the beginning of evolution. Due to the use of NSGA-II (Section 4.3) with 5 coastal sites as  
 6 objectives (Section 3), offspring individuals at generation  $G_t$  must achieve better fitness at at least one of the objectives  
 7 compared to all Pareto-front individuals at  $G_{t-1}$ , thus conserving all site experts (Section 5).

8 Currently, the implementation of ShoreFor as a CGP individual assumes that the equations to calculate  $P$  and  $\Omega$  are  
 9 physical facts and are therefore not included in the CGP-ShoreFor implementation, but rather passed as pre-calculated  
 10 time series.

### 11 4.3. NSGA-II

12 NSGA-II is a well-known and widely used multi-objective genetic algorithm that was proposed in [14]. It makes  
 13 use of the concept of pareto dominance in order to split a population of models into different performance-based  
 14 ranks. A crowding distance measure is also used in order to maintain the diversity of population during evolution. At  
 15 generation  $G_t$ , parents ( $P_t$ ) are selected from the current population using tournament selection and are mutated in  
 16 order to generate a population of offspring models  $Q_t$ . Individuals in  $Q_t$  are evaluated according to the user-defined  
 17 fitness function, then a combined population  $R_t$  is created by merging both  $P_t$  and  $Q_t$ .  $R_t$  is then sorted according based  
 18 on pareto dominance, as well as the crowding distance in lower-ranks, and the  $N$  top-ranking individuals are chosen  
 19 as the upcoming population. The algorithm is run in a loop until a certain threshold is reached, such as the number of  
 20 evaluations executed or a predefined fitness threshold. Due to the elitist nature of NSGA-II, top-ranking models are  
 21 guaranteed to be conserved through the different generations until they are replaced by higher-ranking models. We  
 22 invite the reader to refer to the original work in [14] for further details on the NSGA-II algorithm.

23 Since it's publication, NSGA-II has been applied to a large variety of multi-objective optimization tasks [77, 6,  
 24 15, 69, 80, 52]. In [29], CGP is coupled with a modified version of NSGA-II in order to evolve small mathematical  
 25 expressions and image processing filters and operators. The proposed modified version of NSGA-II is intended to  
 26 reduce the number of fitness evaluations needed to obtain a solution. [25] presents the first use of a multi-objective  
 27 fitness function to improve cartesian genetic programming circuits. The authors make use of NSGA-II as a post-  
 28 processing step to traditional CGP. Functional CGP individuals representing digital circuits are selected at the end of  
 29 evolution and a pareto front is constructed according to three different criteria. In this work, we make use of NSGA-II  
 30 with five fitness dimensions in order to rank our CGP individuals during evolution according to their predictive skills  
 31 at five different coastal sites as presented in Section 3.

### 32 4.4. Fitness evaluation

33 This work makes use of the modified Mielke skill test proposed in [17] in order to evaluate the performance of  
 34 the models. This metric, formulated as  $\lambda$  in Equation 6, is an extension of the Pearson correlation coefficient ( $r$ ) that

1 reduces the value of  $r$  according to the bias between the two datasets. We use this fitness metric as it represents both  
 2 correlation between the target and the forecast as well as the error.

$$\lambda = 1 - \frac{N^{-1} \sum_{i=1}^N (o_i - m_i)^2}{\sigma_o^2 + \sigma_m^2 + (\hat{o} - \hat{m})^2} \quad (6)$$

3 This score is used in order to evaluate the fitness of our CGP individuals over the calibration period during evolution,  
 4 where the objective is to maximize their Mielke score. We also use it to evaluate the forecast performances of the  
 5 individuals after evolution as presented in Section 5.

#### 6 4.5. Model optimization

7 In this work, NSGA-II is used to evolve the CGP-encoded individuals. The algorithm is configured according to  
 8 Table 2 and run for 50 thousand generations. Using NSGA-II,  $N$  offspring are generated each iteration and mixed with  
 9 the previous population of  $P$ , using Pareto dominance to select the next generation. Graphs of  $C$  computational nodes  
 10 are generated and mutated randomly following the mutation rates  $\mu_{nodes}$  and  $\mu_{output}$  for the functional nodes and output  
 11 connections, respectively. This configuration was used for 50 independent trials. All runs were found to converge very  
 12 early on during evolution (within hundreds of generations). After each run, 200 different CGP individuals are recorded  
 13 representing the final generation from that run. The final generations from all runs are grouped into a single merged  
 14 population of 10000 individuals and evaluated using the calibration and forecast datasets. Tables C.1 and C.2 document  
 15 the different functions used in this work, representing the function set used by the genetic algorithm during evolution.

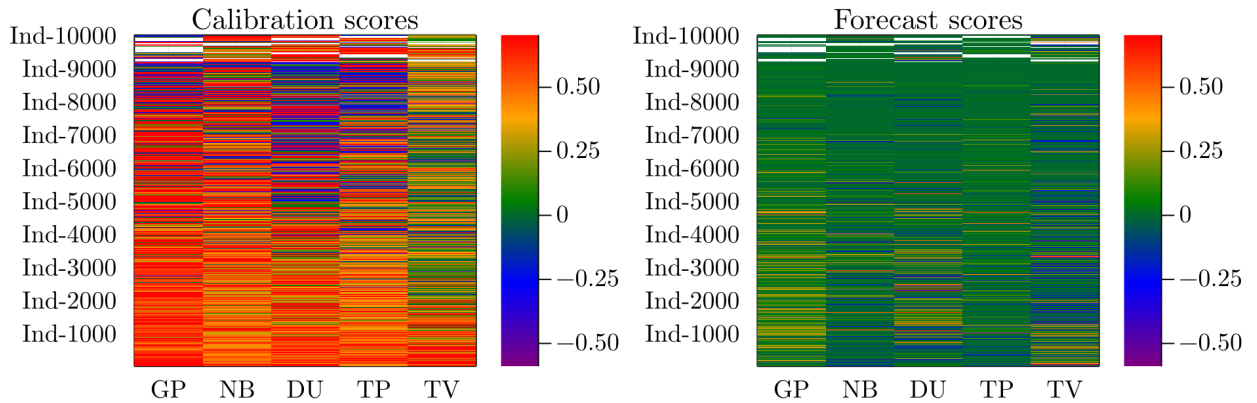


**Figure 3:** Merged population - sorted by mean Mielke score over the calibration period. The color-scale corresponds to the Mielke score.

16 Figures 3 and 4 visualize the performances of the resulting merged population over the calibration and forecast  
 17 periods. Most models are able to achieve a high score over the calibration set, while their performance during the forecast  
 18 period varies between the different sites.

19 In Figure 3, we sort our individuals according to their average Mielke skill score over the 5 sites during the  
 20 calibration period; while Figure 4 visualizes the same result when sorted according to the mean score over the forecast  
 21 period. Interestingly, we find that the highest-performing individuals over the calibration period are not necessarily the  
 22 best-performing models during the forecast period, indicating the tendency of the models to overfit to the calibration  
 23 time series during evolution.

## 24 5. Model analysis

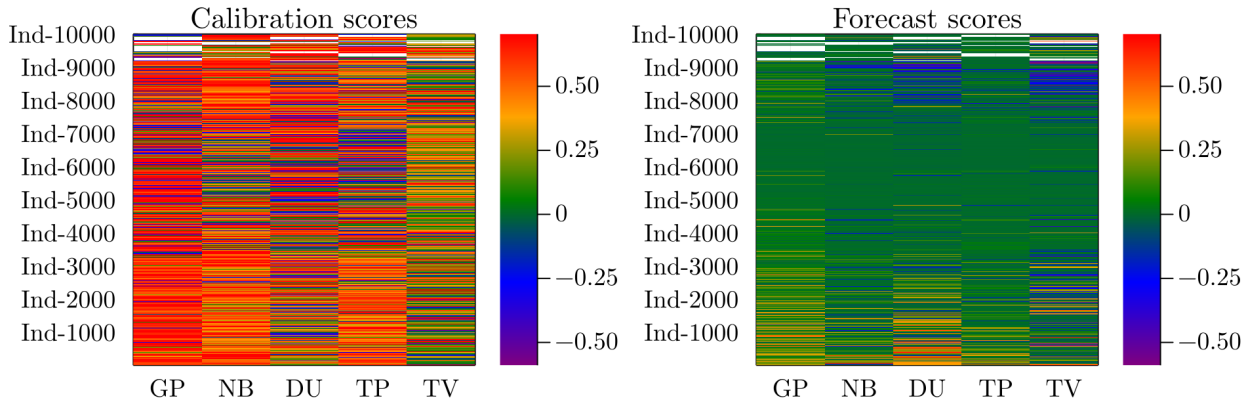
25 We now present and analyze the highest-performing models generated by CGP and NSGA-II using ShoreFor as  
 26 a starting point for evolution. For the purpose of this work, the forecast performance is used in order to select the  
 27 highest-performing individuals for further analysis. Furthermore, models are selected following two different criteria:  
 28 site experts are selected according to their forecast performance at a specific site, and are expected to work best at



**Table 2**

Evolutionary configuration used throughout this work.

Parameter	Value
$P$ population size	200
$N$ offspring	200
$\mu_{nodes}$ mutation rate	0.1
$\mu_{output}$ mutation rate	0.3
$C$ nodes	50

**Figure 4:** Merged population - sorted by mean Mielke score over the forecast period. The color-scale corresponds to the Mielke score.

1 that single site only, whereas generalist models are selected according to their mean Mielke forecast skill over the 5  
2 different sites with the aim of finding a single model that can perform well over all sites.

3 At each site, we present the performances of two site experts and two generalist models and we compare them to  
4 the ground truth data as well as the baseline ShoreFor model. Results on the calibration data used during evolution are  
5 presented in Figure 5 and results on the forecast data are shown in Figure 6. Furthermore, in order to have a deeper  
6 understanding of model performance, we evaluate the performances of our models over isolated trends of different  
7 temporal scales in both the ground truth and predicted time series. This is done using a running mean filter with  
8 varying window sizes corresponding to the target time scale, and a pass-band filter to isolate those time scales. Finally,  
9 Table 3 presents a comparison between the Mielke scores of the evolved expert and generalist models and ShoreFor, and  
10 contextualizes their performances within the current state-of-the-art in data-driven techniques for shoreline forecasting.

11 In general, site experts and generalists are able to achieve a higher Mielke skill score over the calibration period  
12 compared to the ShoreFor model across the five sites. The main improvement over ShoreFor occurs over relatively  
13 shorter-term variations, around five months, as indicated in Figure 5.

14 On the Grand Popo site, the expert models achieve a 20% gain over ShoreFor on the forecast period. The CGP-  
15 expert-GP-1 model shows an improvement in performance over all time scales except over shorter-term variations (1-4  
16 months), whereas CGP-expert-GP-2 achieves a higher skill score over a single dominant time scale (4-12 months).  
17 The generalist models are competitive with ShoreFor while having different behavior, both underperforming at short  
18 timescales but improving for longer timescales.

19 On the Narrabeen dataset, all CGP models achieve a higher Mielke score over both the calibration and forecast  
20 periods. Compared to the results at Narrabeen presented in the original ShoreFor work [13], the base ShoreFor model  
21 achieves a much lower skill score over the forecast period. We presume that this difference is due to the use of a lower  
22 frequency in the dataset; we note that ShoreFor showed high sensitivity to the specific calibration and forecast periods  
23 it was applied at. Compared to ShoreFor, the CGP-expert-NB models demonstrate a significant improvement during  
24 the forecast period, while the two generalist models show a slight improvement.

25 At Duck, all evolved models show a similar behavior of achieving superior Mielke skill at long time scales, while  
26 their performance varies at shorter time scales compared to ShoreFor. All models achieve a higher Mielke skill over

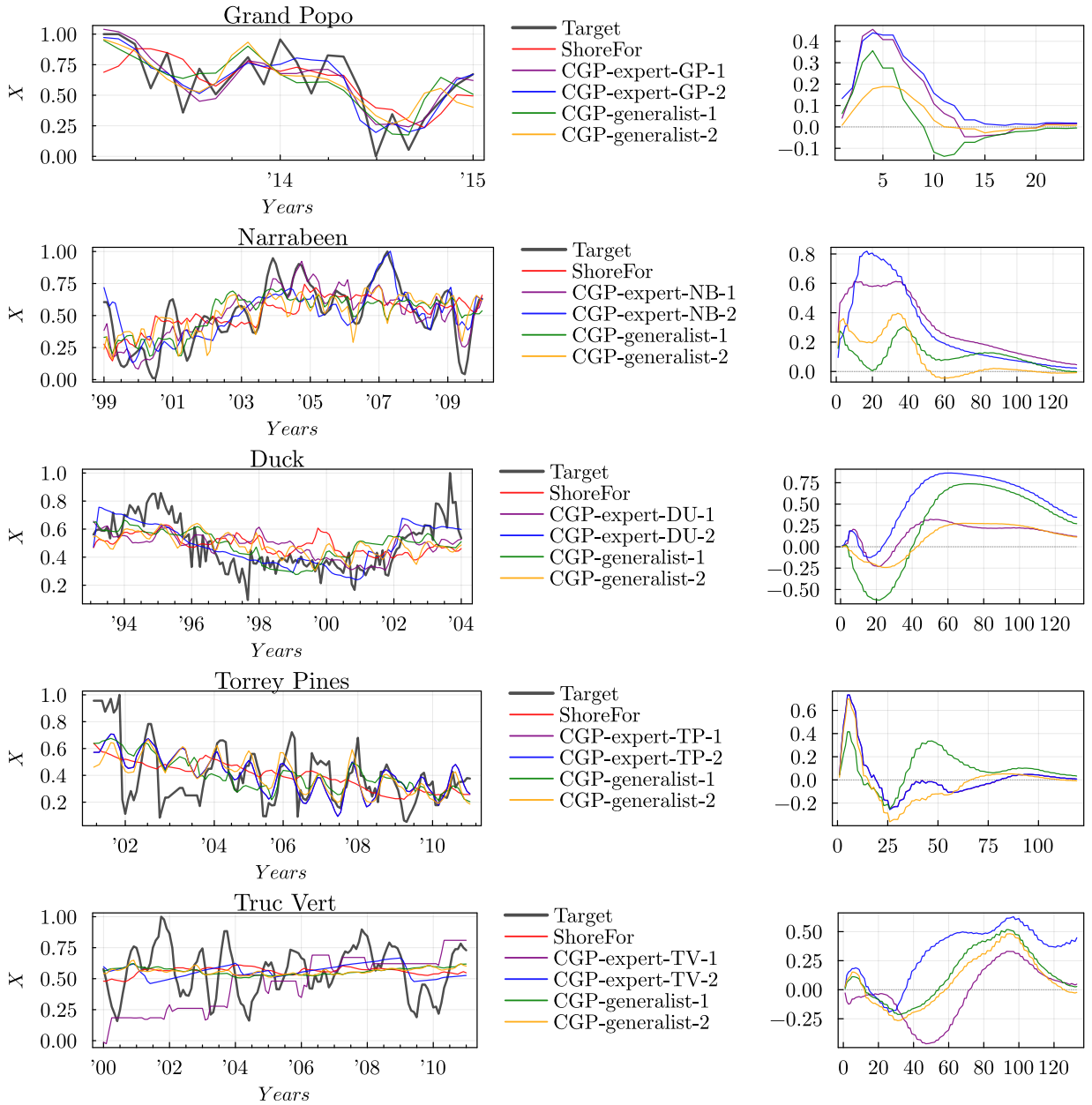


**Figure 5:** Calibration performances on the five sites (left) and the difference in the Mielke skill score at different time scales compared to the performance of ShoreFor at that time scale (Y = 0 represents ShoreFor and the X axis corresponds to the number of months at the evaluated time scale).

- 1 both the calibration and forecast periods except for generalist-2. Compared to ShoreFor, generalist-2 has a lower score
- 2 by 0.02 using the raw model output, while its performance shows a consistent improvement at longer time scales.
- 3 Similarly, on the Torrey Pines dataset, the evolved models improve on ShoreFor on the calibration and forecast
- 4 data; specifically, they capture the strong seasonal cycle better in addition to the long term trend in shoreline position,
- 5 while ShoreFor appears to capture the long term trend only. All models achieve higher skill score using the raw model
- 6 output compared to ShoreFor, and they show a sharp increase in performance at shorter time scales, while the generalist
- 7 models show a decrease in performance at longer scales.

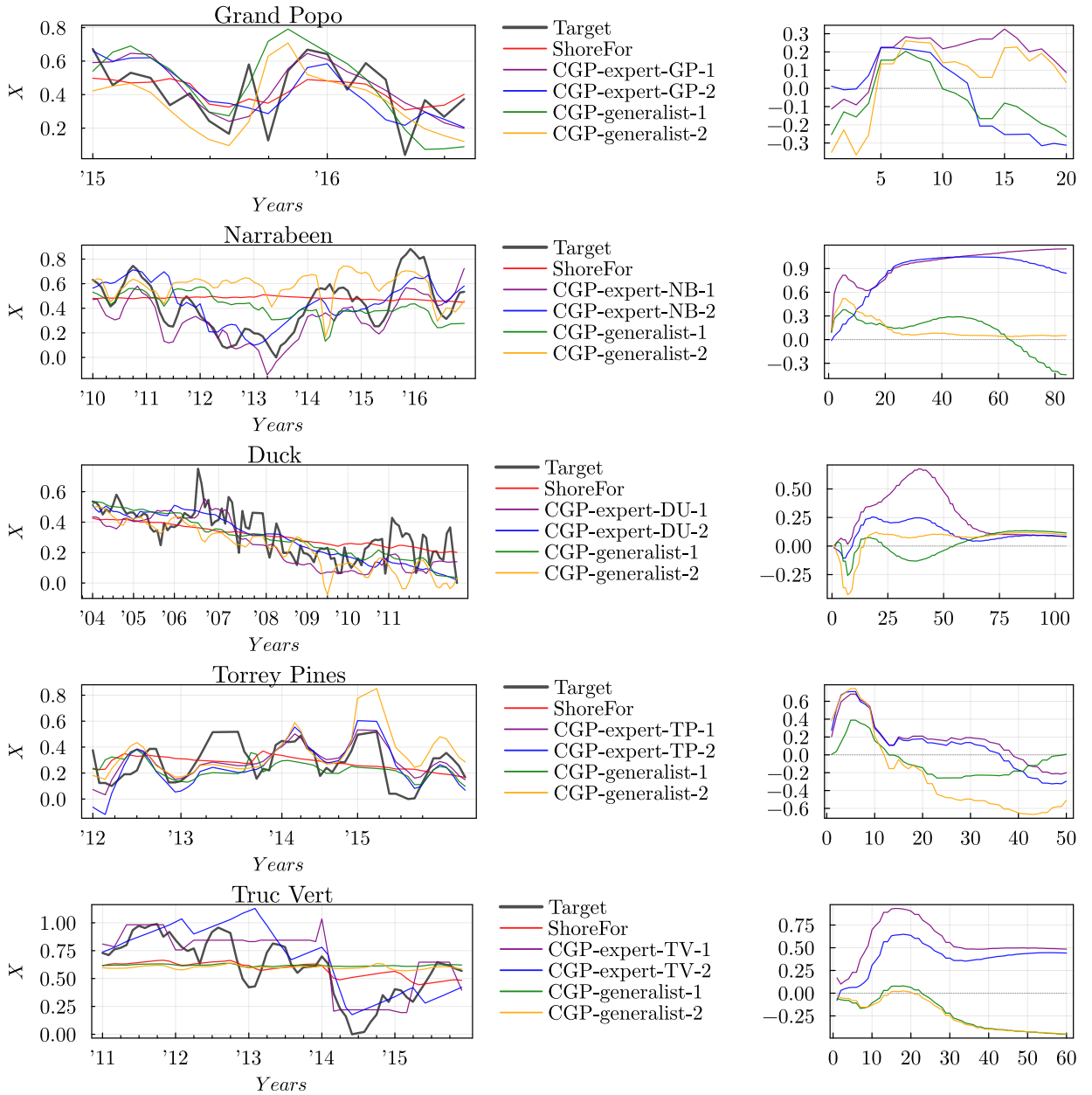


**Figure 6:** Forecast performances on the five sites (left) and the difference in the Mielke skill score at different time scales compared to the performance of ShoreFor at that time scale ( $Y = 0$  represents ShoreFor and the X axis corresponds to the number of months at the evaluated time scale).

1 At Truc Vert, all models fail to produce a reliable forecast of the shoreline position. Compared to ShoreFor, the  
 2 generalist models achieve equivalent performance over the calibration period and are worse at the forecast period;  
 3 as discussed in Section 4.5, models that show high Mielke skill during the calibration period were not necessarily  
 4 well-performing at the forecast period. While the models presented here are selected based on their forecast skill.

5 Overall, the expert models chosen for each site demonstrate large improvements over ShoreFor and high correlation  
 6 with the ground truth forecast data, on which they were not trained. The generalist models perform less well overall, but  
 7 show a consistent improvement over ShoreFor. While specialist models could be trained for a specific site, offering more  
 8 accurate predictions, a general model of shoreline change can be applied globally. We now evaluate the two selected

generalist models to better understand their differences from ShoreFor. The graph representations of the expert models are presented in Appendix B.

Table 3 presents a comparison of the calibration and forecast Mielke scores of ShoreFor to the top expert at each site, in addition to the top generalist model. As discussed in Section 4.5, these models were selected according to their forecast scores. At Grand Popo, most models achieve good Mielke scores over the calibration period, while the GP-expert is the only model to improve on ShoreFor's Mielke score (from 0.51 to 0.63) during the forecast. Similarly, most models calibrate well at Narrabeen while the NB-expert is the only model to demonstrate significant forecast performance (Mielke score of 0.73). At Duck, the generalist model demonstrates the highest calibration Mielke skill of 0.49, while achieving a forecast score competitive with the DU-expert (0.67 compared to 0.7); the generalist and the DU-expert both demonstrate superior performance compared ShoreFor which achieves 0.22 and 0.56 Mielke scores over the calibration and forecast periods, respectively. Multiple models achieve good performance at Torrey Pines during the calibration phase. Interestingly, the DU-expert achieves the highest calibration skill (0.68), while the TP-expert achieves the highest forecast score (0.58). The majority of the models fail to reproduce the shoreline timeseries at Truc Vert. The DU-expert achieves the highest calibration skill (0.62), while the TV-expert is the model with the highest forecast skill score (0.82).

Overall, these results highlight the differences in the applicability of the different expert models, and demonstrate that NSGA-II and CGP can be used to evolve interpretable models that are competitive with the current state-of-the-art among data driven techniques for shoreline forecasting. For example, in [78] different types of neural networks are studied for shoreline forecasting and autoregressive neural networks are reported as the most accurate, with NARNET achieving a MAPE scores of 17.18%, and NARXNET a correlation ( $r$ ) score of 0.26. Additionally, the data-driven techniques tested in [43] include multiple types of neural networks such as MLP, Autoregressive NN, and LSTM, in addition to Bayesian Networks, K-nearest neighbors and Random Forests; using these techniques, the authors report calibration Mielke skills ranging between 0.62 and 0.97, and forecast skills of 0.28-0.46.

## 5.1. Evolved graphs

Figure 7 presents the graph representation of the generalist models discussed in the previous section. Both can also be represented by a system of a equations; the generalist 1 model is equivalent to

$$\frac{dx}{dt} = \begin{cases} \frac{1}{2} \bar{P}^{0.5} \frac{d}{dt} \sqrt{\frac{\phi^2}{2} + \frac{1}{4}(R - \Omega)^2 + S^2}, & \text{if } S \geq P^{0.5} + \Omega \\ 0, & \text{otherwise} \end{cases} \quad (7)$$

and the generalist 2 model to

$$\frac{dx}{dt} = P^{\frac{R}{2}} \frac{d}{dt} 10^S \quad (8)$$

We first note that both models differ largely from the original ShoreFor model. While the fall-velocity  $\Omega$  is used, there is no calculation of an equilibrium term  $\Omega_{eq}$ , and the wave energy flux  $P$  is used directly to calculate  $\frac{dx}{dt}$ , as opposed to calculating accretive and erosive wave forcing terms  $F$ . The combination of information not used in ShoreFor, sea level anomaly  $S$  and river discharge  $R$ , instead determines the influence of wave power on shoreline change. While it is notable that wave power is the primary driver in both evolved models and in ShoreFor, these evolved models offer a different perspective on the relationship between sea level, river discharge, wave power, and shoreline change.

## 6. Discussion

As presented in Figures 3 and 4, we found a large discrepancy in model performance between the calibration and forecast periods. This discrepancy can be attributed to over fitting, a common issue encountered with ML models, including GP, where the models learn to replicate the target training data during evaluation, thereby achieving high performance during training without learning the actual underlying relationships embedded in the training dataset. A possible future direction for this work would be to include the Random Sampling Technique (RST) in the evaluation procedure, where only a random subset of the training dataset is used to compute the fitness of individuals at each

**Table 3**

Comparison of the calibration and forecast performances of ShoreFor, the evolved site experts and the evolved generalist model. The highest Mielke score per site is indicated in **bold**.

Model	$\lambda_{calibration}$						$\lambda_{forecast}$					
	GP	NB	DU	TP	TV	$\bar{\lambda}_c$	GP	NB	DU	TP	TV	$\bar{\lambda}_f$
ShoreFor	0.65	0.44	0.22	0.36	0.05	0.34	0.51	-0.04	0.56	0.14	0.34	0.3
CGP-generalist-1	0.73	0.56	<b>0.49</b>	0.48	0.05	0.46	0.51	0.11	0.67	0.23	0.06	<b>0.32</b>
CGP-expert-GP-1	<b>0.82</b>	0.67	-0.24	0.45	0.17	0.37	<b>0.63</b>	0.0	-0.13	0.13	-0.1	0.11
CGP-expert-NB-1	0.66	<b>0.81</b>	0.14	0.35	0.09	0.41	0.23	<b>0.73</b>	0.05	0.06	-0.04	0.21
CGP-expert-DU-1	0.71	0.6	0.38	<b>0.68</b>	<b>0.62</b>	<b>0.6</b>	0.03	-0.0	<b>0.7</b>	0.0	0.3	0.21
CGP-expert-TP-1	0.63	0.8	0.13	0.58	0.05	0.44	0.31	0.17	0.15	<b>0.58</b>	-0.0	0.24
CGP-expert-TV-1	0.8	0.62	-0.15	0.55	0.0	0.36	0.2	-0.18	-0.08	0.44	<b>0.82</b>	0.24

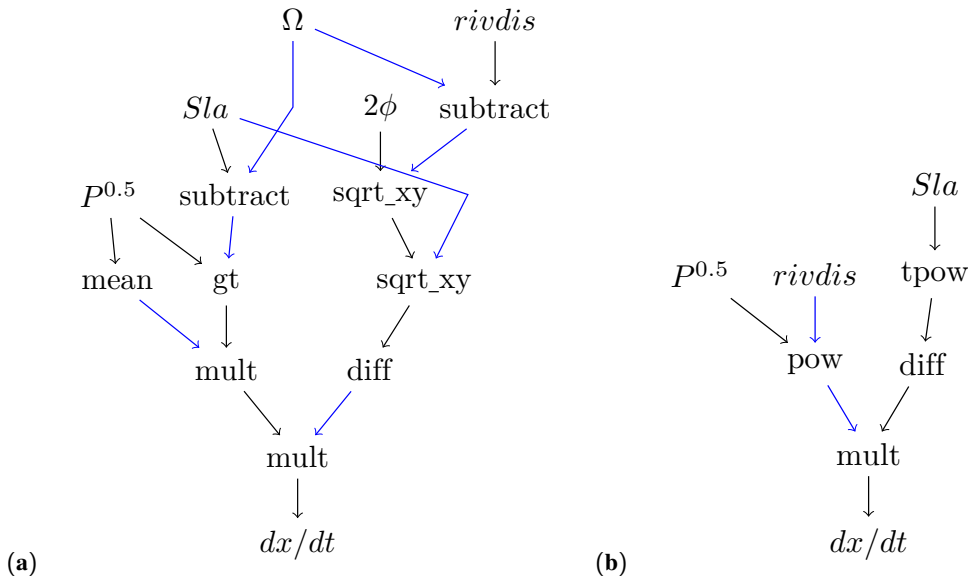


**Figure 7:** The (a) generalist-1 and (b) generalist-2 models produced by CGP and NSGA-II using ShoreFor as the starting point for evolution.

1 generation. RST was first proposed in [19] in order to reduce the computational resources required to run GP. Later  
 2 works demonstrated promising results on the use of RST as a method for improving model generalization in GP  
 3 [32, 36, 23]. In the context of this work, RST could be used to select random periods from each time series in order  
 4 to test model performance during evolution, taking into account the physical signification of the selected periods and  
 5 their lengths. Another possible approach to increasing model generalization and algorithm efficiency, especially in  
 6 cases where larger datasets are available, is the use of a data balancing technique such as [68].

7 Another future direction would be to include shoreline data from Satellite Image Time Series datasets, using a tool  
 8 such as [16] for example, in order to enlarge the coverage of the different sites into coastal zones. The availability of  
 9 such a dataset would allow for the use of a more globally-representative set of coastal zones to be used for calibration  
 10 during evolution. It would also allow for a more exhaustive set of test areas after evolution. We believe that such  
 11 modifications would greatly increase the algorithm's ability to produce more robust generalist models.

12 An interesting pattern found during this work is the tendency of the evolved models to degrade the performance of  
 13 the baseline ShoreFor model at certain time scales (see Figures 5 and 6). One possible way to overcome this degradation  
 14 would be to set the different time scales (event-scale, seasonal, interannual, decadal) as the objectives for evolution.

15 Furthermore, this work did not explore the effects of different CGP mutation schemes such as node addition and  
 16 deletion, in addition to different crossover operations. However, we believe that it could be interesting to explore

1 such operations, especially considering the possibility of including other shoreline forecasting systems into the initial  
2 gene-pool of the algorithm.

## 3 7. Conclusion

4 In this work, we have presented our experiments on the use of CGP and NSGA-II in order to evolve a pre-established  
5 shoreline forecasting model, ShoreFor. CGP was used in order to encode the ShoreFor system of equations into a format  
6 that can be evolved using evolutionary algorithms. During evolution, NSGA-II is employed in order to maintain a  
7 pareto-front of optimal solutions according to their performances at five different coastal points from around the globe.

8 On a population-level, a discrepancy was found between the training and test performances of the evolved models.  
9 We believe that the inclusion of additional coastal sites in addition to longer shoreline time series would allow for more  
10 sophisticated experimentation on the use of the Random Sampling Technique to increase model generalization.

11 The evolved models were presented from two different perspectives. Expert models are site-specific experts that  
12 are selected according to the highest forecast score at a specific site. These models were found to achieve a higher  
13 skill score compared to the baseline ShoreFor model over all sites, during both the calibration and forecast periods.  
14 On the other hand, generalist models are selected according to their average forecast skill score over the five different  
15 objectives. The generalist models achieve similar or higher performance than that of ShoreFor over four of the five  
16 sites used in this work.

17 Overall, the results presented in this work are a strong motivation for further study on the use of genetic  
18 programming and multi-objective genetic algorithms in shoreline forecasting studies due to the wide potential  
19 applicability of the evolved models and their interpretability as ordinary systems of equations.

## 20 Software and Data Availability

21 This work was developed in the Julia programming language (version 1.6.1). We make use of the evolutionary  
22 computation frameworks CartesianGeneticProgramming.jl and Cambrian.jl originally implemented by D. G. Wilson  
23 and adapted by M. Al Najar for this work. The software used to produce this work can be found under an Apache  
24 V2 license at: <https://github.com/mahmoud-al-najar/CGP-ShoreFor>, in addition to further details on the  
25 packages required to reproduce the work. The datasets used here originate from a number of related works. Data  
26 for Grand Popo, Narrabeen, Torrey Pines, Truc Vert were gathered from [1, 62, 37, 8], respectively. Additionally, data  
27 covering Duck was obtained from the U.S. Army Engineer Research & Development Centre, Coast & Hydraulics  
28 Laboratory, Field Research Facility<sup>1</sup>. The CGP-ShoreFor GitHub repository additionally provides the processed data  
29 compiled from each source's raw data presented in this work.

## 30 Acknowledgements

31 M. Al Najar is currently supported by the CNES (Centre national d'études spatiales) and the Occitanie Region as  
32 part of M. Al Najar's thesis contract. All experiments were conducted on the CNES HPC cluster HAL.

## 33 References

- 34 [1] Abessolo, G., Almar, R., Jouanno, J., Bonou, F., Castelle, B., Larson, M., 2020. Beach adaptation to intraseasonal sea level changes.  
35 Environmental Research Communications 2, 051003.
- 36 [2] Al Najar, M., Almar, R., Bergsma, E.W.J., Delvit, J.M., Wilson, D.G., 2022. Genetic improvement of shoreline evolution forecasting models,  
37 in: Proceedings of the Genetic and Evolutionary Computation Conference Companion, Association for Computing Machinery, New York,  
38 NY, USA. p. 1916–1923. URL: <https://doi.org/10.1145/3520304.3534041>, doi:10.1145/3520304.3534041.
- 39 [3] Almar, R., Ranasinghe, R., Sénéchal, N., Bonneton, P., Roelvink, D., Bryan, K.R., Marieu, V., Parisot, J.P., 2012. Video-based detection of  
40 shorelines at complex meso–macro tidal beaches. Journal of Coastal Research 28, 1040–1048.
- 41 [4] Angelov, P.P., Soares, E.A., Jiang, R., Arnold, N.I., Atkinson, P.M., 2021. Explainable artificial intelligence: an analytical review. Wiley  
42 Interdisciplinary Reviews: Data Mining and Knowledge Discovery 11, e1424.
- 43 [5] Bonou, F., Angnuureng, D.B., Sohou, Z., Almar, R., Alory, G., du Penhoat, Y., 2018. Shoreline and beach cusps dynamics at the low tide  
44 terraced grand popo beach, bénin (west africa): A statistical approach. Journal of Coastal Research , 138–144.
- 45 [6] Brownlee, A.E., Wright, J.A., 2015. Constrained, mixed-integer and multi-objective optimisation of building designs by nsga-ii with fitness  
46 approximation. Applied Soft Computing 33, 114–126.

<sup>1</sup><https://chlthredds.erdc.dren.mil/thredds/catalog/frf/catalog.html>

- [7] Calkoen, F., Luijendijk, A., Rivero, C.R., Kras, E., Baart, F., 2021. Traditional vs. machine-learning methods for forecasting sandy shoreline evolution using historic satellite-derived shorelines. *Remote Sensing* 13, 934.
- [8] Castelle, B., Bujan, S., Marieu, V., Ferreira, S., 2020. 16 years of topographic surveys of rip-channelled high-energy meso-macrotidal sandy beach. *Scientific Data* 7, 410.
- [9] Češka, M., Matyáš, J., Mrazek, V., Sekanina, L., Vasicek, Z., Vojnar, T., 2017. Approximating complex arithmetic circuits with formal error guarantees: 32-bit multipliers accomplished, in: 2017 IEEE/ACM International Conference on Computer-Aided Design (ICCAD), IEEE. pp. 416–423.
- [10] Church, J.A., White, N.J., 2006. A 20th century acceleration in global sea-level rise. *Geophysical research letters* 33.
- [11] Cranmer, K., Bowman, R.S., 2005. Physicsgp: A genetic programming approach to event selection. *Computer Physics Communications* 167, 165–176.
- [12] Davidson, M., 2021. Forecasting coastal evolution on time-scales of days to decades. *Coastal Engineering* 168, 103928.
- [13] Davidson, M., Splinter, K., Turner, I., 2013. A simple equilibrium model for predicting shoreline change. *Coastal Engineering* 73, 191–202.
- [14] Deb, K., Pratap, A., Agarwal, S., Meyarivan, T., 2002. A fast and elitist multiobjective genetic algorithm: Nsga-ii. *IEEE transactions on evolutionary computation* 6, 182–197.
- [15] Delgarm, N., Sajadi, B., Delgarm, S., Kowsary, F., 2016. A novel approach for the simulation-based optimization of the buildings energy consumption using nsga-ii: Case study in iran. *Energy and Buildings* 127, 552–560.
- [16] Doherty, Y., Harley, M.D., Vos, K., Splinter, K.D., 2022. A python toolkit to monitor sandy shoreline change using high-resolution planetscope cubesats. *Environmental Modelling & Software* 157, 105512.
- [17] Duveiller, G., Fasbender, D., Meroni, M., 2016. Revisiting the concept of a symmetric index of agreement for continuous datasets. *Scientific reports* 6, 1–14.
- [18] Friedel, M.J., 2011. A data-driven approach for modeling post-fire debris-flow volumes and their uncertainty. *Environmental Modelling & Software* 26, 1583–1598.
- [19] Gathercole, C., Ross, P., 1994. Dynamic training subset selection for supervised learning in genetic programming, in: *International Conference on Parallel Problem Solving from Nature*, Springer. pp. 312–321.
- [20] Gaur, S., Deo, M., 2008. Real-time wave forecasting using genetic programming. *Ocean engineering* 35, 1166–1172.
- [21] Goldstein, E.B., Coco, G., Murray, A.B., 2013. Prediction of wave ripple characteristics using genetic programming. *Continental Shelf Research* 71, 1–15.
- [22] Goldstein, E.B., Coco, G., Plant, N.G., 2019. A review of machine learning applications to coastal sediment transport and morphodynamics. *Earth-science reviews* 194, 97–108.
- [23] Gonçalves, I., Silva, S., Melo, J.B., Carreiras, J., 2012. Random sampling technique for overfitting control in genetic programming, in: *European Conference on Genetic Programming*, Springer. pp. 218–229.
- [24] Harding, S., Leitner, J., Schmidhuber, J., 2013. Cartesian genetic programming for image processing, in: *Genetic programming theory and practice X*. Springer, pp. 31–44.
- [25] Hilder, J., Walker, J.A., Tyrrell, A., 2010. Use of a multi-objective fitness function to improve cartesian genetic programming circuits, in: 2010 NASA/ESA Conference on Adaptive Hardware and Systems, IEEE. pp. 179–185.
- [26] Ibaceta, R., Splinter, K.D., Harley, M.D., Turner, I.L., 2022. Improving multi-decadal coastal shoreline change predictions by including model parameter non-stationarity. *Frontiers in Marine Science* 9, 1012041.
- [27] Itzkin, M., Moore, L.J., Ruggiero, P., Hovenga, P.A., Hacker, S.D., 2022. Combining process-based and data-driven approaches to forecast beach and dune change. *Environmental Modelling & Software* 153, 105404.
- [28] Kabliman, E., Kolody, A.H., Kronsteiner, J., Kommenda, M., Kronberger, G., 2021. Application of symbolic regression for constitutive modeling of plastic deformation. *Applications in Engineering Science* 6, 100052.
- [29] Kalkreuth, R., Rudolph, G., Krone, J., 2016. More efficient evolution of small genetic programs in cartesian genetic programming by using genotype age, in: 2016 IEEE Congress on Evolutionary Computation (CEC), IEEE. pp. 5052–5059.
- [30] Kambekar, A., Deo, M., 2012. Wave prediction using genetic programming and model trees. *Journal of Coastal Research* 28, 43–50.
- [31] La Cava, W., Orzechowski, P., Burlacu, B., de Franca, F.O., Virgolin, M., Jin, Y., Kommenda, M., Moore, J.H., 2021. Contemporary symbolic regression methods and their relative performance, in: *Thirty-fifth Conference on Neural Information Processing Systems Datasets and Benchmarks Track (Round 1)*.
- [32] Langdon, W., 2011. Minimising testing in genetic programming. *RN* 11, 1.
- [33] Le Cozannet, G., Bulteau, T., Castelle, B., Ranasinghe, R., Wöppelmann, G., Rohmer, J., Bernon, N., Idier, D., Louisor, J., Salas-y Méria, D., 2019. Quantifying uncertainties of sandy shoreline change projections as sea level rises. *Scientific reports* 9, 1–11.
- [34] Lesser, G.R., Roelvink, J.v., van Kester, J.T.M., Stelling, G., 2004. Development and validation of a three-dimensional morphological model. *Coastal engineering* 51, 883–915.
- [35] Link, J., Yager, P., Anjos, J., Bediaga, I., Castromonte, C., Göbel, C., Machado, A., Magnin, J., Massafferri, A., De Miranda, J., et al., 2005. Application of genetic programming to high energy physics event selection. *Nuclear Instruments and Methods in Physics Research Section A: Accelerators, Spectrometers, Detectors and Associated Equipment* 551, 504–527.
- [36] Liu, Y., Khoshgoftaar, T., 2004. Reducing overfitting in genetic programming models for software quality classification, in: *Eighth IEEE International Symposium on High Assurance Systems Engineering*, 2004. Proceedings., IEEE Computer Society. pp. 56–65.
- [37] Ludka, B.C., Guza, R., O'Reilly, W., Merrifield, M., Flick, R., Bak, A.S., Hesser, T., Bucciarelli, R., Olfe, C., Woodward, B., et al., 2019. Sixteen years of bathymetry and waves at san diego beaches. *Scientific data* 6, 161.
- [38] Makkeasorn, A., Chang, N.B., Zhou, X., 2008. Short-term streamflow forecasting with global climate change implications—a comparative study between genetic programming and neural network models. *Journal of Hydrology* 352, 336–354.
- [39] Marchesiello, P., Chauchat, J., Shafiei, H., Almar, R., Benshila, R., Dumas, F., Debreu, L., 2022. 3d wave-resolving simulation of sandbar migration. *Ocean Modelling*, 102127.

- [40] Mehr, A.D., Nourani, V., 2017. A pareto-optimal moving average-multigene genetic programming model for rainfall-runoff modelling. *Environmental modelling & software* 92, 239–251.
- [41] Miller, J.F., 2011. Cartesian genetic programming, in: *Cartesian Genetic Programming*. Springer, pp. 17–34.
- [42] Miller, J.F., 2020. Cartesian genetic programming: its status and future. *Genetic Programming and Evolvable Machines* 21, 129–168.
- [43] Montaña, J., Coco, G., Antolínez, J.A., Beuzen, T., Bryan, K.R., Cagigal, L., Castelle, B., Davidson, M.A., Goldstein, E.B., Ibaceta, R., et al., 2020. Blind testing of shoreline evolution models. *Scientific reports* 10, 1–10.
- [44] Nicholls, R.J., Hanson, S.E., Lowe, J.A., Warrick, R.A., Lu, X., Long, A.J., 2014. Sea-level scenarios for evaluating coastal impacts. *Wiley Interdisciplinary Reviews: Climate Change* 5, 129–150.
- [45] Orzechowski, P., La Cava, W., Moore, J.H., 2018. Where are we now? a large benchmark study of recent symbolic regression methods, in: *Proceedings of the Genetic and Evolutionary Computation Conference*, pp. 1183–1190.
- [46] Passarella, M., Goldstein, E.B., De Muro, S., Coco, G., 2018. The use of genetic programming to develop a predictor of swash excursion on sandy beaches. *Natural Hazards and Earth System Sciences* 18, 599–611.
- [47] Quade, M., Abel, M., Shafi, K., Niven, R.K., Noack, B.R., 2016. Prediction of dynamical systems by symbolic regression. *Physical Review E* 94, 012214.
- [48] Reguero, B.G., Losada, I.J., Méndez, F.J., 2019. A recent increase in global wave power as a consequence of oceanic warming. *Nature communications* 10, 1–14.
- [49] Robinet, A., Idier, D., Castelle, B., Marieu, V., 2018. A reduced-complexity shoreline change model combining longshore and cross-shore processes: The lx-shore model. *Environmental modelling & software* 109, 1–16.
- [50] Schepper, R., Almar, R., Bergsma, E., de Vries, S., Reniers, A., Davidson, M., Splinter, K., 2021. Modelling cross-shore shoreline change on multiple timescales and their interactions. *Journal of Marine Science and Engineering* 9, 582.
- [51] Sekanina, L., Harding, S.L., Banzhaf, W., Kowaliw, T., 2011. Image processing and cgp, in: *Cartesian genetic programming*. Springer, pp. 181–215.
- [52] Shi, S., Ge, Y., Chen, L., Feng, H., 2020. Four-objective optimization of irreversible atkinson cycle based on nsga-ii. *Entropy* 22, 1150.
- [53] Simmons, J.A., Splinter, K.D., 2022. A multi-model ensemble approach to coastal storm erosion prediction. *Environmental Modelling & Software* 150, 105356.
- [54] Spector, L., Barnum, H., Bernstein, H.J., Swamy, N., 1999. Quantum computing applications of genetic programming. *Advances in genetic programming* 3, 135–160.
- [55] Spector, L., Klein, J., 2008. Machine invention of quantum computing circuits by means of genetic programming. *AI EDAM* 22, 275–283.
- [56] Splinter, K.D., Turner, I.L., Davidson, M.A., Barnard, P., Castelle, B., Oltman-Shay, J., 2014. A generalized equilibrium model for predicting daily to interannual shoreline response. *Journal of Geophysical Research: Earth Surface* 119, 1936–1958.
- [57] Tjoa, E., Guan, C., 2020. A survey on explainable artificial intelligence (xai): Toward medical xai. *IEEE transactions on neural networks and learning systems* 32, 4793–4813.
- [58] Toimil, A., Losada, I.J., Camus, P., Díaz-Simal, P., 2017. Managing coastal erosion under climate change at the regional scale. *Coastal Engineering* 128, 106–122.
- [59] Tran, Y.H., Barthélemy, E., 2020. Combined longshore and cross-shore shoreline model for closed embayed beaches. *Coastal Engineering* 158, 103692.
- [60] Tran, Y.H., Marchesiello, P., Almar, R., Ho, D.T., Nguyen, T., Thuan, D.H., Barthélemy, E., 2021. Combined longshore and cross-shore modeling for low-energy embayed sandy beaches. *Journal of Marine Science and Engineering* 9, 979.
- [61] Turki, I., Medina, R., Coco, G., Gonzalez, M., 2013. An equilibrium model to predict shoreline rotation of pocket beaches. *Marine Geology* 346, 220–232.
- [62] Turner, I.L., Harley, M.D., Short, A.D., Simmons, J.A., Bracs, M.A., Phillips, M.S., Splinter, K.D., 2016. A multi-decade dataset of monthly beach profile surveys and inshore wave forcing at narrabeen, australia. *Scientific data* 3, 1–13.
- [63] Udrescu, S.M., Tan, A., Feng, J., Neto, O., Wu, T., Tegmark, M., 2020. Ai feynman 2.0: Pareto-optimal symbolic regression exploiting graph modularity. *Advances in Neural Information Processing Systems* 33, 4860–4871.
- [64] Udrescu, S.M., Tegmark, M., 2020. Ai feynman: A physics-inspired method for symbolic regression. *Science Advances* 6, eaay2631.
- [65] Uriot, T., Virgolin, M., Alderliesten, T., Bosman, P.A., 2022. On genetic programming representations and fitness functions for interpretable dimensionality reduction, in: *Proceedings of the Genetic and Evolutionary Computation Conference*, pp. 458–466.
- [66] Vaddirreddy, H., Rasheed, A., Staples, A.E., San, O., 2020. Feature engineering and symbolic regression methods for detecting hidden physics from sparse sensor observation data. *Physics of Fluids* 32, 015113.
- [67] Vitousek, S., Barnard, P.L., Limber, P., Erikson, L., Cole, B., 2017. A model integrating longshore and cross-shore processes for predicting long-term shoreline response to climate change. *Journal of Geophysical Research: Earth Surface* 122, 782–806.
- [68] Vladislavleva, E., Smits, G., Den Hertog, D., 2009. On the importance of data balancing for symbolic regression. *IEEE Transactions on Evolutionary Computation* 14, 252–277.
- [69] Wang, S., Zhao, D., Yuan, J., Li, H., Gao, Y., 2019a. Application of nsga-ii algorithm for fault diagnosis in power system. *Electric Power Systems Research* 175, 105893.
- [70] Wang, Y., Wagner, N., Rondinelli, J.M., 2019b. Symbolic regression in materials science. *MRS Communications* 9, 793–805.
- [71] Warner, J.C., Sherwood, C.R., Signell, R.P., Harris, C.K., Arango, H.G., 2008. Development of a three-dimensional, regional, coupled wave, current, and sediment-transport model. *Computers & geosciences* 34, 1284–1306.
- [72] Warren, I., Bach, H., 1992. Mike 21: a modelling system for estuaries, coastal waters and seas. *Environmental Software* 7, 229–240.
- [73] Weng, B., Song, Z., Zhu, R., Yan, Q., Sun, Q., Grice, C.G., Yan, Y., Yin, W.J., 2020. Simple descriptor derived from symbolic regression accelerating the discovery of new perovskite catalysts. *Nature communications* 11, 1–8.
- [74] Wilson, D.G., Cussat-Blanc, S., Luga, H., Miller, J.F., 2018. Evolving simple programs for playing atari games, in: *Proceedings of the Genetic and Evolutionary Computation Conference*, pp. 229–236.



- 1 [75] Wright, L.D., Short, A.D., Green, M., 1985. Short-term changes in the morphodynamic states of beaches and surf zones: an empirical predictive  
2 model. *Marine geology* 62, 339–364.
- 3 [76] Yin, C., Anh, D.T., Mai, S.T., Le, A., Nguyen, V.H., Nguyen, V.C., Tinh, N.X., Tanaka, H., Viet, N.T., Nguyen, L.D., et al., 2021. Advanced  
4 machine learning techniques for predicting nha trang shorelines. *IEEE Access* 9, 98132–98149.
- 5 [77] Yusoff, Y., Ngadiman, M.S., Zain, A.M., 2011. Overview of nsga-ii for optimizing machining process parameters. *Procedia Engineering* 15,  
6 3978–3983.
- 7 [78] Zeinali, S., Dehghani, M., Talebbeydokhti, N., 2021. Artificial neural network for the prediction of shoreline changes in narrabeen, australia.  
8 *Applied Ocean Research* 107, 102362.
- 9 [79] Zerenner, T., Venema, V., Friederichs, P., Simmer, C., 2017. Downscaling near-surface atmospheric fields with multi-objective genetic  
10 programming, in: *Proceedings of the Genetic and Evolutionary Computation Conference Companion*, pp. 11–12.
- 11 [80] Zhang, L., Chen, L., Xia, S., Ge, Y., Wang, C., Feng, H., 2020. Multi-objective optimization for helium-heated reverse water gas shift reactor  
12 by using nsga-ii. *International Journal of Heat and Mass Transfer* 148, 119025.

1 A. CGP-ShoreFor graph

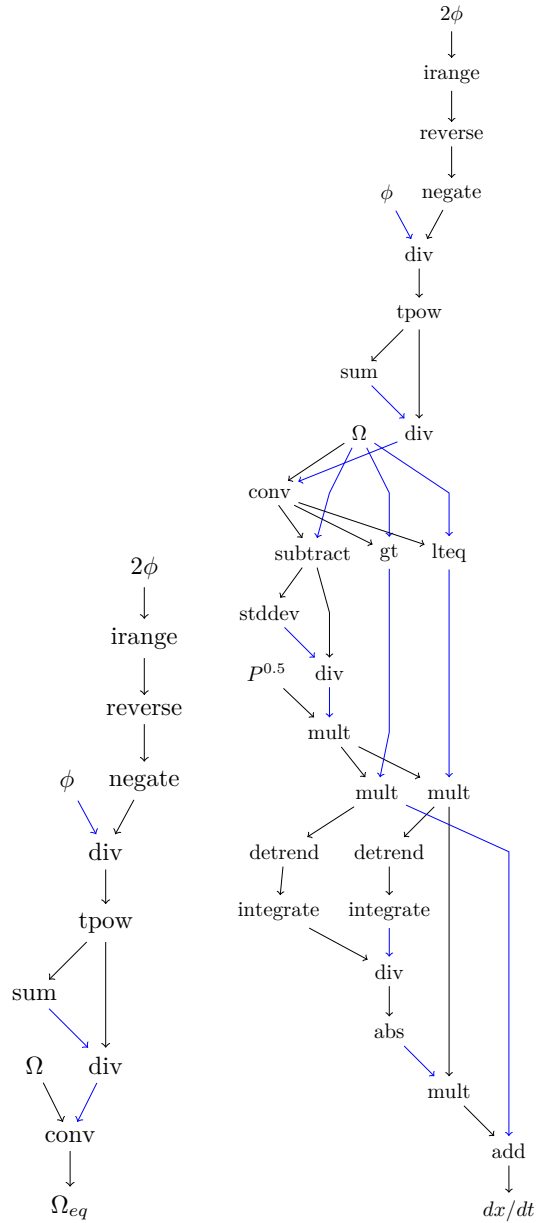
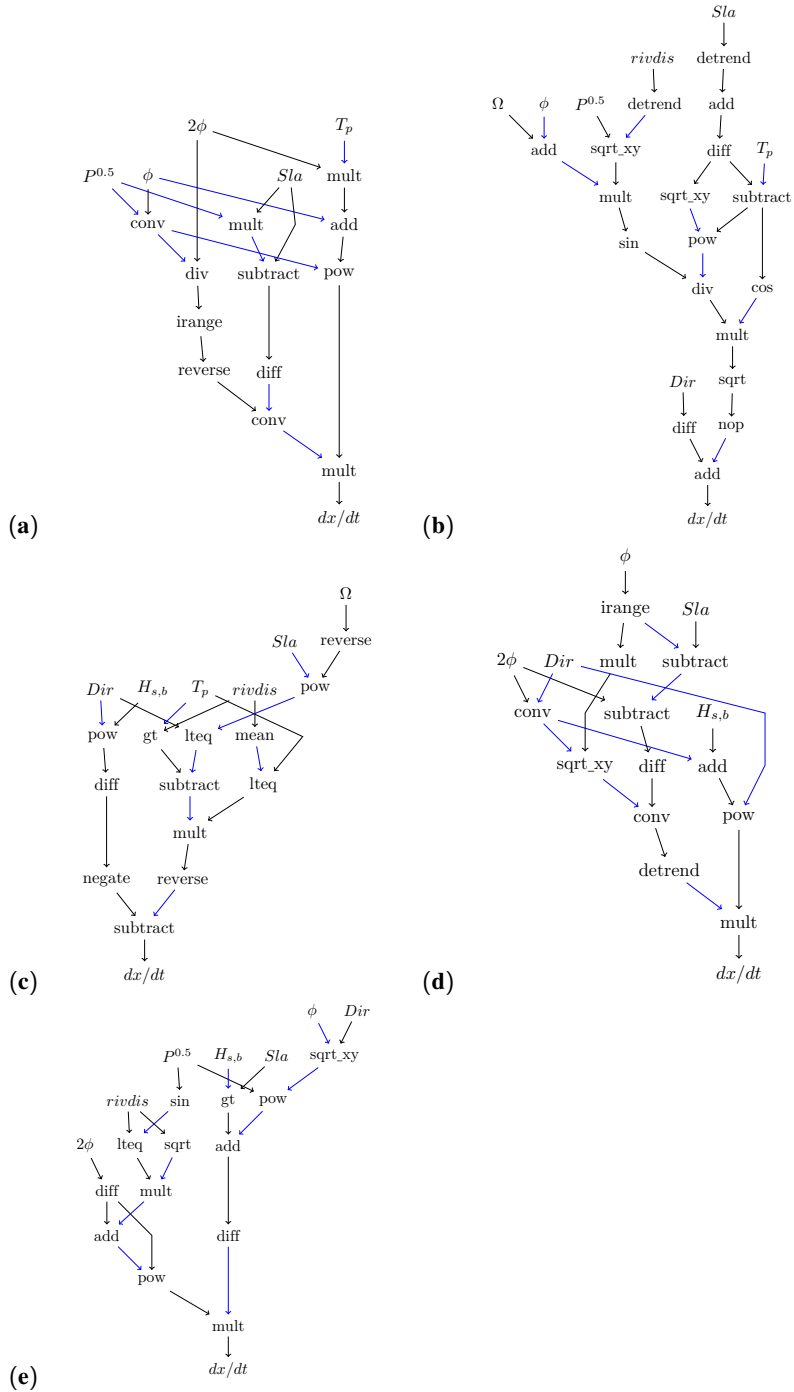


Figure A.1: Graph representations of the  $\Omega_{eq}$  equation (left) and the full ShoreFor system of equations (right).

1 **B. Expert graphs**



**Figure B.2:** The evolved expert models with the highest forecast performance scores presented in Section 5. (a) CGP-expert-GP-1, (b) CGP-expert-NB-1, (c) CGP-expert-DU-1, (d) CGP-expert-TP-1 (e) CGP-expert-TV-1.

2 **C. Function set**

**Table C.1**

The set of scalar operations included in the GA's function set.

Function	Operation
abs	$ x $
sqrt	$\sqrt{x}$
sin	$\sin x$
cos	$\cos x$
negate	$-x$
tpow	$10^x$
nop	$x$
add	$x + y$
subtract	$x - y$
mult	$x * y$
div	$x \div y$
pow	$x^y$
sqrt_xy	$\sqrt{x^2 + y^2}$
lteq	$x \leq y$
gt	$x > y$

**Table C.2**

The set of vector operations included in the GA's function set. \* Assuming a constant time step in the time series.

Function	Operation
diff	$x_i = x_i - x_{i-1}$
sum	$\sum_{i=1}^n x$
stddev	$\sigma x$
detrend	$\langle x \rangle$
integrate*	$\int_a^b f(x)dx \approx \sum_{i=1}^n \frac{f(x_{i-1})+f(x_i)}{2} \Delta x_i$
mean	$\frac{1}{n} \sum_{i=1}^n x$
reverse	$reverse(x)$
irange	$[1, 2, 3...n], n = length(x)$
conv	$conv(x, y)$